Development of Control Method for Abration and Evaluation of Electrocautery Device Controller

JungHun Choi*

Department of Mechanical Engineering, Georgia Southern University

Abstract: The symmetrical impedance bridge, will be suggested to yield consistent and reliable results for measuring tissue damage during electrosurgical ablation. The methods that were identified as potentially viable for ablation detection were force and displacement measurements between the electrode tip and tissue surface. These were found to correlate tissue damage due to a high degree of variability in charge density caused by contact area variation. Another method, temperature measurement via thermistors, will be found to have a response time and a non-contact method will be examined with the size constraints. The last method will be to measure and correlate changes in the power output of the ESU to tissue damage. This method will be practically examined to measure and correlate to tissue damage due to ESU power output modulation. The changes in the tissue's electrical properties can be measured directly far more easily than measuring the power output. Correlation with tissue damage tended to be strong with an error range below what can be detectable by the human eye. But the high degree of variability in the mechanical properties of tissue makes the use of force and displacement measurements difficult to implement as part of a control method for ablation control.

Keywords: Electrocautery, Polyp, Biopsy Forceps, Colonoscope.

1. INTRODUCTION

Colorectal cancer is one of the most deadly forms of cancer domestically and worldwide – killing an estimated 50,000 people per year in the US alone [1]. As with all types of cancers, early detection plays a critical role in patient survival, and screening is recommended for everyone typically starting between the ages of 45 and 50 years old - perhaps earlier depending on the individual's risk factors. Screening continues indefinitely at a frequency largely depending on the patient's risk factors and the biopsy results taken during previous screenings. Colonoscopy has become the standard method for screening for colorectal cancer, which consists of taking random tissue biopsies and inspecting the colon wall visually for irregular growths termed, polyps. These polyps are the origin of colorectal cancer and ultimately need to be removed; however, this removal process is complicated by the size and shape of the polyp. Shown in Figure **1**, are two different types of polyps exist: sessile and pedunculated.

The most common polyp found is called a sessile polyp and is the most difficult type to remove because they lay flat against the colon wall [2]. Generally speaking, these sessile polyps are removed by use of electrosurgical ablation with hot biopsy forceps. This electrosurgical ablation removes these sessile polyps by burning the tissue away by passing a high-frequency alternating current through the tissue volume of interest, as shown in Figure **2**.

This electrosurgical ablation creates two regions of tissue damage: the core and white peripheral crest,

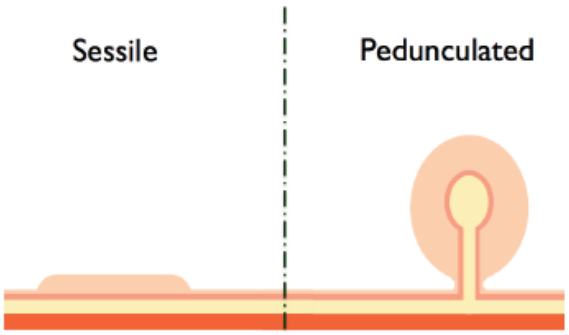

Figure 1: Two categories of polyp shape: sessile and pedunculated.

shown in Figure **3**. The surgeon has very poor control over the amount of tissue ablated. The only indication of the amount ablation is the growth the white peripheral crest propagating outward from the center of the ablation site - caused by the denaturing of the proteins when frictionally heated. The surgeon uses the colonoscope's camera to visually inspect the propagation rate of the white peripheral crest, which complicates determining the amount of tissue damage because the white peripheral crest size is distorted because of the two-dimensional video image.

This poor control over the level of ablation leads to serious complications. Perforation of the colon wall is the most serious. According to data collected during the Munich Polypectomy Study, perforation carries a 5% mortality rate and occurs at a rate of 1.1% [3]. It should be noted that data regarding the actual perforation and mortality rate is difficult to obtain for two reasons. First, some U.S. surgeons are not required to report perforations [3]. Second, delayed perforations can occur a week after the actual surgery, which can lead to patient death and is often overlooked in many patients - particularly elderly patients [4]. Finally, the

*Address correspondence to this author at the Department of Mechanical Engineering, Georgia Southern University;
E-mail: jchoi@georgiasouthern.edu

E-ISSN: 2409-9848/24

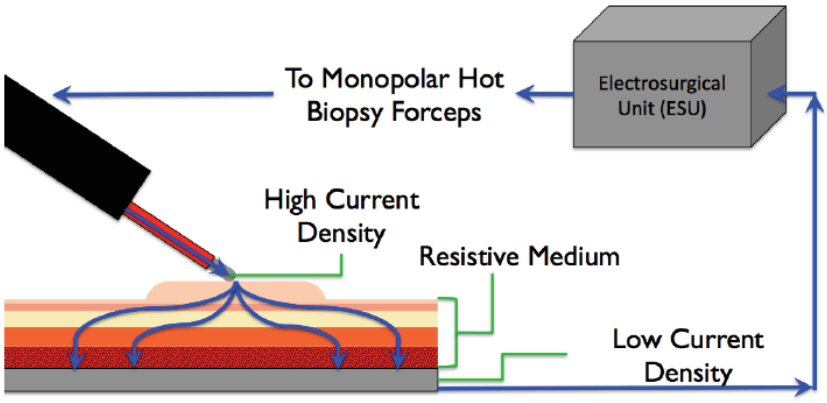

Figure 2: Electrosurgery Ablation of Sessile Polyps.

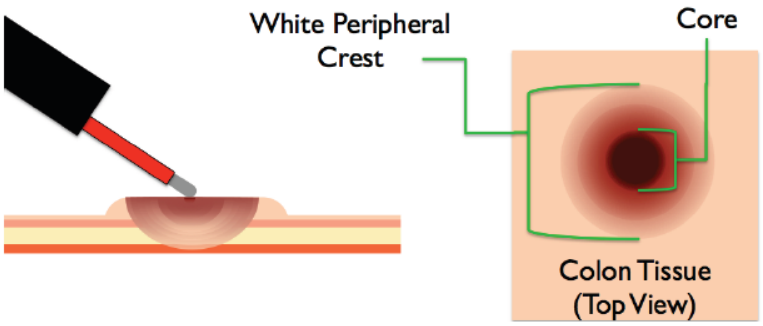

Figure 3: Ablation Tissue Damage Regions: Core and White Peripheral Crest.

complication rate from the Munich Polypectomy Study had an overall complication rate of 9.7% [3]. The complications ranged from bleeding to Postpolypectomy syndrome, both known to be caused by excessive ablation [3, 5].

Given the fact that everyone is recommended to undergo colorectal cancer screening and the fact that 9.7% of those people will encounter some type of complication that has a high probability of being connected to poor ablation control. A system should be developed to effectively control the amount of ablation. Careful consideration should be given to minimize disruption and ensure a swift adoption and integration into existing equipment. Shown in Figure **4**, are two pictures and an illustration showing the spatial challenges with integrating a control system within existing colonoscopes.

The approach will be to experimentally relate the power consumed by the tissue and changes in the electrical properties of the tissue to the degree of tissue damage sustained. Factors that govern electrosurgical ablation will be identified and subsequently evaluated for potential in an ablation control system. Standard methods by which to measure these factors will be identified and implemented as a series of preliminary experiments to systematically evaluate the most promising methods. Correlation of the power consumed; electrical changes of the tissue;

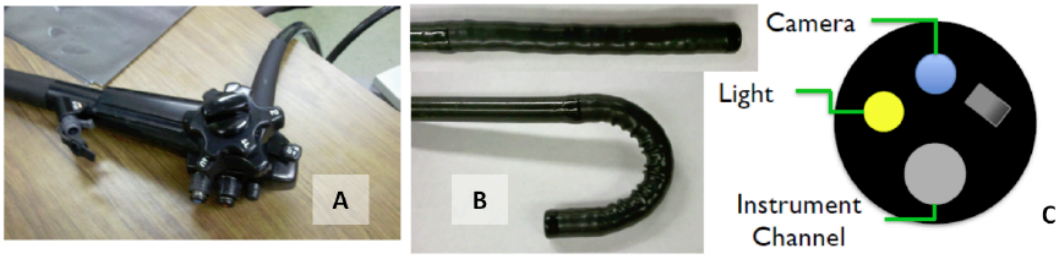

Figure 4: Colonoscope control handle (**A**), flexile distal tip (**B**), and typical arrangement of components (**C**).

temperature change; contact surface area; and the duration of ablation will be related to the amount and type of tissue damage sustained. Final evaluation of the control systems performance will be evaluated by a working prototype.

2. BACKGROUND

Generally speaking, electrosurgery can be broken into two categories: monopolar or bipolar electrosurgery. In monopolar electrosurgery, the alternating current flows between the active and returned electrode (or neutral electrode), which is placed on the patient's leg or buttocks. Intense heat is generated when the resistance of the tissue impedes the flow of electric current. The peak voltage and current density govern the electrosurgical effect. Slow heating of the tissue can produce a coagulation effect, which is achieved by keeping the peak voltage below 200 V and decreasing the duty cycle of the waveform. A rapid heating of the tissue can produce a cutting effect, which is achieved by increasing the peak voltage to over 200 V and increasing the duty cycle of the waveform. The surface area of the tissue in contact with active electrode changes the current density and the resulting electrosurgical effect. For instance, the greater the surface area in contact with the electrode, the lower the current density. With monopolar electrosurgery, the return electrode must have a much larger surface area in contact with the patient's body then the active electrode to ensure burns do not occur at the return electrode pad. In recent years, return electrode pads have been designed so that ESU's can monitor the impedance of the return electrode pad and ensure that the contact surface area is large enough. Additionally, the ESU's modulate the power output in order to account for the rapid increase in the tissue's impedance caused by the thermal damage during electrosurgery [5].

In bipolar electrosurgery, the active and return electrodes are both located on the instrument. This change eliminates the need for a return electrode pad. Additionally, thermal damage is limited to the tissue between the two electrodes [6]. The principles governing the end-results of waveform modulation are identical for both bipolar and monopolar electrosurgery, but the ESU does not generate identical waveforms for both monopolar and bipolar electrosurgery.

2.1. Current Density

Controlling the current density as a function of time and voltage controls the therapeutic effect during electrosurgery. The amount of surface area in contact with the active electrode directly influences the amount of current density [7]. As the total surface area in contact with the active electrode increases, the current density decreases, and visa versa. Subsequently, the amount of thermal heating is directly proportional to the current density. Resistive heating is thought to be the major thermal mechanism responsible for this phenomenon. By varying the duty cycle of the current flow, subsequently affecting the current density, a variety of therapeutic effects can be achieved [8]. Additionally, varying the peak voltage changes the resulting therapeutic effects. Electrosurgery is possible at peak voltages equal to or greater then 200V. By balancing the value of the peak voltage and duty cycle, various therapeutic affects can be achieved. A schematic is shown below in Figure **5**, illustrating this rate of heating dependency [9].

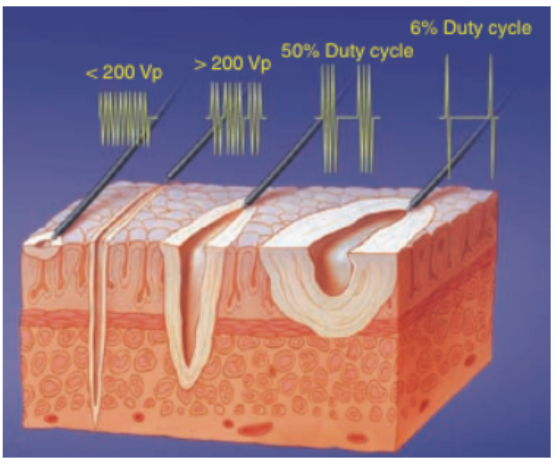

Figure 5: Schematic of the effect of varying waveforms [9].

2.2. Thermodynamic Mechanisms

Explanations of the thermal mechanisms that are ultimately responsible for tissue damage are studied from the cellular and molecular level. At the cellular level, the flowing electrical energy is impeded (resisted) by the tissue, which results in an energy conversion to thermal energy. This resistive heating is complicated by the high frequencies at which electrosurgical instruments operate. At the molecular level, frictional heating is thought to occur due to interaction between the electric field and charges in the aqueous solution of the intracellular space. Finally, both of these thermal mechanisms are dependent upon the rate of electrical energy delivered to the tissue and the rate of temperature change of the tissue. Stated another way, delivering an equal amount of energy to tissue does not yield the same amount of thermal damage.

Resistive Heating

Resistive heating occurs at the cellular level when the tissue impedes (resists) the flow of the alternating current. At this point the electrical energy is transferred into thermal energy. This resistive heating is complicated by the high frequencies at which

electrosurgical instruments operate. When high frequency currents flow around a conductor, a local current flow can be set up within that conductor [10]. This current flow within the conductor can cause two separate problems: eddy current heating and electrostatic pick-up. In the case of eddy current heating, the current flow within the conductor translates into resistive heating. In the case of electrostatic pick-up, the current flow within the conductor can reach a voltage potential high enough to cause electric arcing. Since tissue is a non-homogeneous material comprising of substances with a wide variety of resistance values, determining the amount of resistive heating becomes a complicated problem. However, simplifications have been made to approximate the electrical equivalent circuit of tissues. In Figure **6**, a schematic of this circuit is shown below [10].

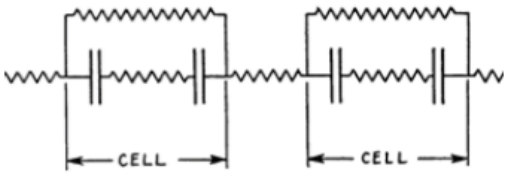

Figure 6: Electrical Model of Tissue [10].

Frictional Heating

Frictional heating during electrosurgery is thought to be the result of the interaction between the electric field and the intracellular fluid. At this cellular level, partial charges found on molecular dipoles and free ions follow the change in direction of the alternating current creating translational movement and frictional heat [11]. This thermal mechanism helps to explain the collateral damage that is characteristic of electrosurgery because the thermal energy is generated from within intracellular spaces and not from the electrode [11].

Heat Rate Dependence of Protein Denaturing

Fully quantifying biological tissue damage as a function of both temperature and time remains unsolved. Conditions within the tissue's extracellular and intracellular spaces are random and in a state of continuous change in an effort to maintain homeostasis. Both thermal mechanisms described above, resistive and frictional heating, are ultimately dependent on the rate of heating. However, another thermal mechanism considers the molecular reactions, which occur as a result of the combination of resistive and frictional heating.

During electrosurgery, the flowing electric current induces many complicated reactions between molecules, each with its own unique rate constant. However, partial quantifications have been introduced which approximates these unique rate constants into a single rate constant [12]. This can then be used to define an arbitrary function of tissue injury as a function of temperature:

$$\Omega(t) = \int_0^t A \cdot e^{\frac{-\Delta E}{R \cdot T}} \cdot dt \tag{1}$$

where *T* is the temperature (K) calculated at each point of the model region, *R* is the gas constant 8.314 (J/mole · K), *A* is the frequency factor (s^{-1}), and ΔE is the activation energy for protein dissociation (J/mole). For values greater than 1 for Ω, the thermal damage to the tissue is irreversible [13].

2.3. Heat Transfer

To analytically model the heat transfer in tissue the bioheat equation, developed by Penne, is modified to add additional heat sources [12,14,15,16,17]. The modified bioheat equation is expressed as:

$$pc\frac{\partial T}{\partial t} = k\nabla^2 + w_b c_b (T - T_a) + q_m + q_g \tag{2}$$

where ρ is the tissue density (kg/m^3), c is the heat capacity $(J/(kg \cdot K^\circ))$, and is the thermal conductivity $(W/(m \cdot K^\circ))$. is the effective blood perfusion parameter $(kg/m^3 \cdot s)$. is the blood heat capacity $(J/(kg \cdot K^\circ))$. is the local tissue temperature $(^\circ\mathrm{C})$, is the blood inlet temperature $(^\circ\mathrm{C})$, which is also assumed to be the steady-state temperature of the tissue. is the energy generated by metabolic processes (W/m^3), and is neglected since the energy generated during electrosurgical ablation is much larger. is the external heat generation rate from the electrosurgical instrument (W/m^3). is the time [14].

2.4. Current Flow

To analytically model the electric field in the tissue, a quasistatic electrical conduction model is applied across the frequency range of 300 kHz – 1MHz. At these frequencies, the wavelength of the electrical current is much larger then the electrode size, which limits the energy generated to a small volume around the tip of the instrument's electrode. Subsequently, displacement currents can be ignored, leading to the expression for the energy of the heat source as:

$$q_g = \mathbf{J} \cdot \mathbf{E} \tag{3}$$

where is the current density $(\mathrm{A/m^2})$ and E is the electric field intensity (V/m). The values of these two vectors can then be evaluated using Laplace's equation:

$$\nabla[\sigma(T)\nabla V] = 0 \tag{4}$$

where is the voltage calculated by taking the root mean square of the electrosurgical waveform and σ is the electrical conductivity $(\mathrm{S/m})$.

From the bioheat transfer equation (Eq. 2) and the electric field equation (Eq. 4), we see that electrical conductivity of tissue is a function of both temperature and position, which requires that both of these equations be solved simultaneously through iterative computation.

To determine electrical conductivity as a function of temperature, Schwan *et al* developed a standard increase of 2%, which can be expressed lineally as [15]:

$$\sigma(T) = \sigma_{T_{ref}}\left(1 + 0.02\left(T - T_{ref}\right)\right) \tag{5}$$

where T_{ref} is the baseline temperature for electrical conductivity, and $\sigma_{T_{ref}}$ is found from known electrical properties of tissue [15].

To determine the thermal conductivity as a function of temperature, Valvano *et al.* developed a linear relation expressed as [16]:

$$k(T) = k_{T_{ref}} + 0.0013\left(T - T_{ref}\right) \tag{6}$$

where T_{ref} is found from known thermal conductivity properties of tissue [17].

2.5. Limitations of a Numerical Approach

The energy exchange between the blood and tissue is modeled as a non-directional heat source. Pennes model assumes that heat is transferred between the tissue and blood at the capillary bed. Concerns with this assumption arise from the belief that thermal equilibrium occurs either before or after the capillary bed. The heat lost in the pre-capillary bed would be much smaller then the heat lost in the post-capillary bed – due to the rate of blood flow being smaller in the pre-capillary bed and the rate of blood flow being higher in the post-capillary bed. This also assumes that no large blood vessels are in near the area of thermal ablation [16]. Although it is well known that the physical properties of biological tissue, particularly electrical conductivity, rapidly change as a function of temperature, there is limited information regarding terms to compensate for this phenomenon with regard to the bioheat equation. This limits the usefulness of the bioheat equation to temperatures below 100. Above this temperature formation of gas and protein dissociation complicate the quantification [16].

Gross simplifications can be made to characterize both the heat transfer and thermal mechanisms that ultimately lead to models that closely match experimental data. The bioheat transfer equation can be modified in various ways to describe changes in the thermal profile of tissue as flowing current is converted into thermal energy. Likewise, the electrical field can be effectively modeled as it flows through the tissue volume. However, these heat transfer models seem to be limited to conditions in which the tissue is fully characterized.

Similarly, the thermal mechanisms seem to effectively describe the governing factors of electrosurgery at a fundamental level. For resistive heating, we have seen that tissue can be approximated as an electrical circuit, but the high frequency creates two problems related to current flows within conductors of the tissue. The first problem arises from these stray current flows creating additional and unpredictable heating within tissues. The second problems arises from these stray current flows building up voltage potentials that can reach levels where arcing occurs. Predicting the amount of resistive heating remains an impossible task from a practical standpoint. Frictional heating has shown that charges within the intracellular space can interact with the changing electrical field yielding in an additional thermal mechanism. Both of these mechanisms are dependent on the rate of heating, but a third thermal mechanism helps to describe protein denaturation as a function of the rate of heating. Owing to the vast number of reactions possible, each with its own unique rate constant, an arbitrary function has been developed to approximate these reactions. Varying the heating rate of the current density results in a variety of therapeutic affects, which seem to be the resulting combination of the three thermal mechanisms: resistive heating, frictional heating, and heat rate dependency of protein denaturing. However, the degree at which these three thermal mechanisms are participating during electrosurgery seems to be largely unknown.

These models describe a small portion of the problem - how tissue changes under known conditions. A numerical approach would need to extend the models to include a numerical model of the sensor's response. Since no experimental data exists regarding how the sensor responds, the numerical results would still need to be validated by experimental data. The most effective method to evaluate the sensor's ability to detect tissue damage is by collecting experimental data. Also, experimental approach provides an opportunity to evaluate practical aspects of the sensors that would

otherwise be hidden in a numerical approach. Although the heat transfer models seem to be limited to idealized conditions, they are still useful as a tool for validating the experimental results and ultimately to develop control logic.

3. PRELIMINARY STUDIES

Controlling the lesion size of electrosurgical ablation within the large intestine remains a problem of implementing practical methods and components within the endoscopic system. Traditional methods for control rely on components that are too large, not cost-effective, or have a slow response. Thus, to systematically evaluate the feasibility of methods to control the lesion size from electrosurgical ablation a primarily experimental approach chosen. Practical aspects such as speed, noise, and reliability – would otherwise be invisible from a numerical approach. Preliminary studies have been conducted to systematically evaluate method feasibility and to validate the method's results.

3.1. Variable Assessment of Monopolar Hot Biopsy Forceps

The primary aim was to assess and correlate tissue damage from MHBF based on five key factors: ESU power mode selected; electrode displacement with respect to the endoscope; load of the electrode acting normal to the tissue's surface; peak power consumed by the ESU; and duration of ablation. The secondary aim was to evaluate the feasibility of these methods for use within an ablation control system. The amount of tissue damage, for both the core and white peripheral crest regions, were expected to show strong correlations to each of the four key factors; however, there was only a weak correlation to the tissue damage located within the white peripheral crest region. The amount of tissue damage within the core region remained constant and independent of the four key factors. It was speculated to be the result of the electrode's displacement being constant throughout ablation. Stated another way, had the electrode been permitted to increase it's displacement during ablation, the core size would have increased as well. Moreover, tissue damage for both regions was quantified by visually inspecting photos of the ablation sites. This two dimensional quantification of tissue damage omitted the depth of the tissue damage for both regions; however, the white peripheral crest would still be detected on the surface as protein denaturing continues to propagate through molecular frictional heating. Unlike the core, which vaporizes tissues primarily though resistive heating of tissue within close proximity of the electrode and does not propagate. The secondary outcome was that these methods did not lend themselves as feasible methods for ablation control due to the weak correlation with the amount of tissue damage and the practical difficulty with implementing the corresponding sensors as part of a control system.

3.2. Methods

An *ex vivo* model was developed for the evaluation of the hot biopsy forceps based closely on similar *in vivo* studies [4, 18]. The overall experimental set-up is shown in Figure **7**. The experimental fixture rigidly held the endoscope normal to the surface of the tissue and the hot biopsy forceps were allowed to pass through the endoscope's working channel. Goat colon samples were fixed on a bed of ground beef, which acted as a resistive medium to electrically represent the human

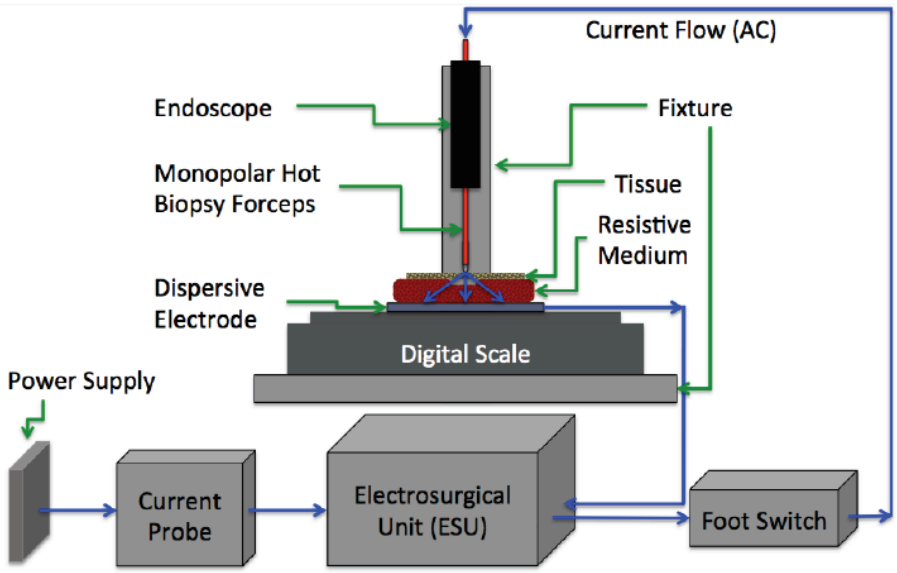

Figure 7: Study 1 - Experimental Set-Up.

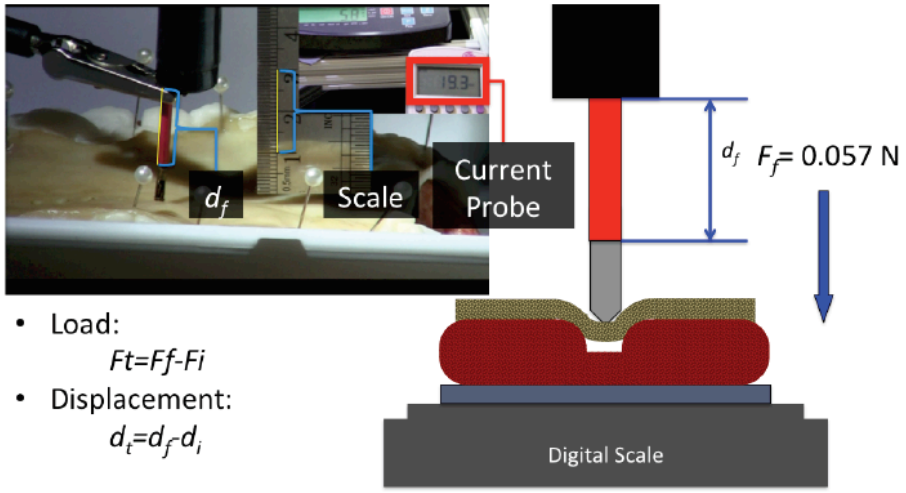

Figure 8: Example of the Methods for measuring Power Consumption, Displacement and Force.

body. Ablation was carried out with standard Hot Biopsy forceps and an Electrosurgical Unit (ESU). The power mode was selected as pure cut, which generates a purely sinusoidal waveform and were selected as either low (30W), medium (60W), or high (90W). Four parameters were measured throughout the evaluation: duration of ablation; displacement of tissue; peak power consumption of the ESU; and load of the electrode normal to the surface of the tissue. The duration of ablation was measured by using a video camera to record the ablation event and the footage was reviewed to determine the duration of the ablation events. The ESU was manually triggered using a foot-pedal and the duration of ablation was approximated during the experiment as short, medium and long. A current probe, connected in series, measured the peak power consumption of the ESU during ablation.

The electrode's displacement relative to the end of the endoscope's tip was measured by visually inspecting photo's taken before and after displacement had occurred. A ruler was used as a known scale, and the photo's were analyzed using ImageJ software. The load of the electrode acting normal to the surface of the tissue was measured by using a digital scale. An example of the methods for measuring the peak power consumption, displacement, and load are shown in Figure **8**.

The amount of tissue damage was quantified by photographing the ablation sites with a known scale in the frame. The size of the ablation sites were analyzed with ImageJ software to determine the surface area of the white peripheral crest and core, an example is shown in Figure **9**.

4. RESULTS AND DISCUSSION

The surface area of the core and white peripheral crest compared to displacement are shown in Figure **10**. The surface area of the core shows a high degree of variation and a weak trend regarding increased surface area with respect to increased displacement. The surface area of the white peripheral crest also shows a high degree of variation, but shows a trend regarding increased surface area with respect to increased displacement. At the high power mode (90W), increased surface area with respect to increased displacement was smaller then the other

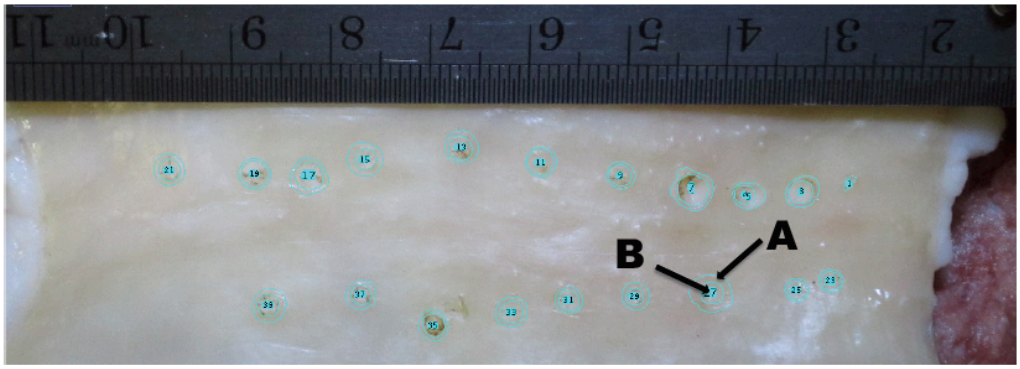

Figure 9: Ablation and analysis sites for the **A**) White Peripheral Crest and **B**) Core.

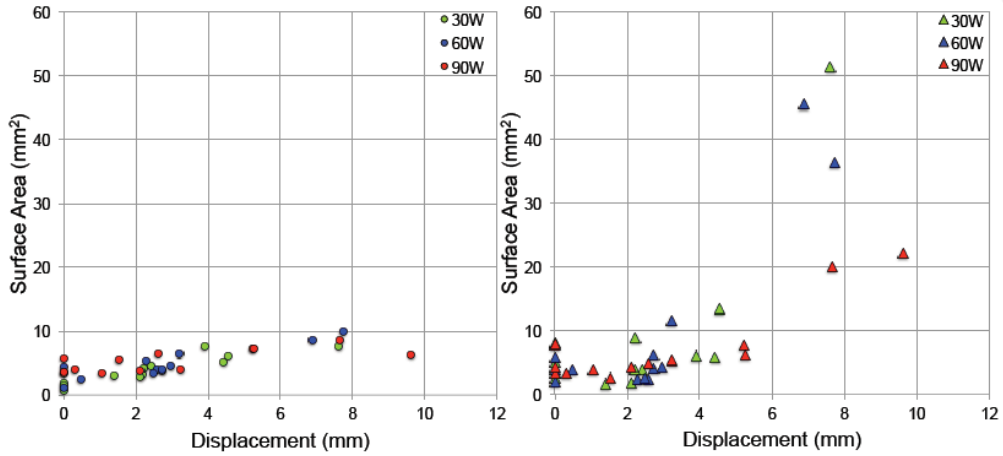

Figure 10: Surface Area of damaged tissue compared with Displacement (mm) of electrode for (**A**) Core and (**B**) White Peripheral Crest.

power modes (30W and 60W) but had a smaller variation. The surface area of the core shows no strong trend with respect to any of the power modes and increased displacement.

The surface area of the core compared to the load, shown in Figure **11**, shows similar trends as with the displacement: high degree of variability with no apparent trend with respect to increased load or power modes, 30 60 or 90W. The surface area of the white peripheral crest compared to the load, also shown in Figure **11**, shows a high degree of variability and a weak trend regarding increased surface area with respect to increased load. Similar to the comparison to displacement, at the high power mode (90W), there is a smaller degree of variability and a stronger trend with respect to increased surface area and increased load when compared to the two other power modes (30W and 60W). Additionally, the high power mode (90W), yields smaller increases in surface area with respect to increased load, when compared to the two other power modes (30W and 60W). The surface area is generally larger for the low power mode (30W) with respect to the load. The medium power mode (60W), generally yields medium surface area when compared to the two other power modes (30W and 90W), with respect to increased load.

The surface area of the core compared to the peak power consumed, shown in Figure **12**, shows a similarly high degree of variability as shown in the displacement and load results. There seems to be no strong correlation between increased peak power consumption and increase surface area of the core. The low power mode (30W), yielded higher values for the peak power consumption when compared to the other two power modes (60W and 90W). The surface area of the white peripheral crest compared to the peak power consumption, also shown in Figure **12**, shows a high degree of variability and a weak trend regarding increased surface area with respect to increased peak power consumption. Unlike the comparisons for displacement and load, at the low power mode (30W), there is a smaller degree of variability and a stronger trend with respect to increased surface area and increased load when compared to the two other power modes (60W and 90W). Additionally, the low power mode (30W), yields larger increases in surface area of

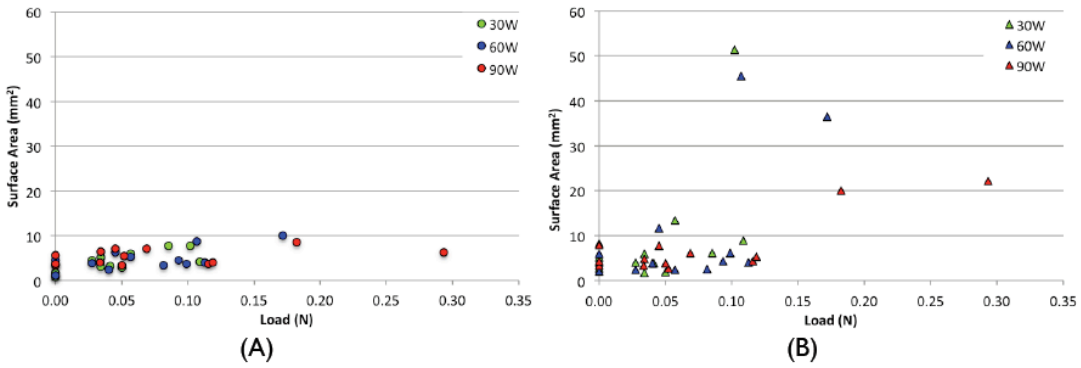

Figure 11: Surface Area of damaged tissue compared with Static Load (N) of electrode for (**A**) Core and (**B**) White Peripheral Crest.

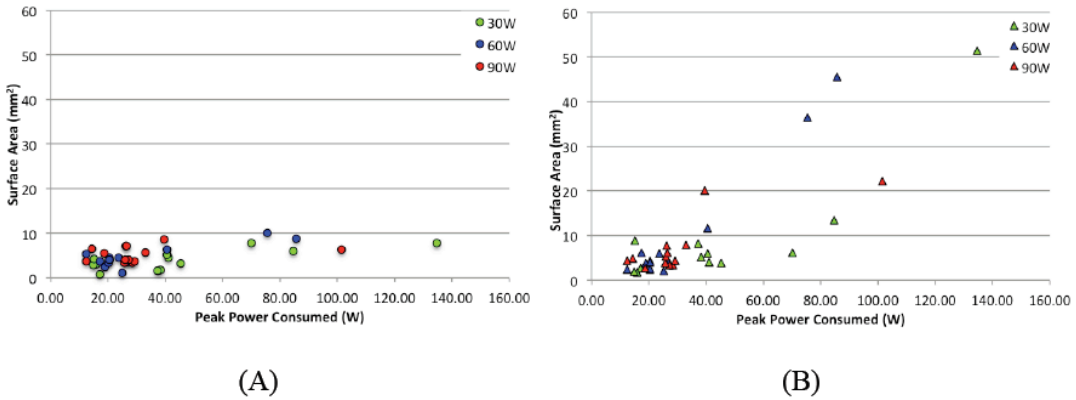

Figure 12: Surface Area of damaged tissue compared with Peak Power Consumed (W) by the ESU for (**A**) Core and (**B**) White Peripheral Crest.

the white peripheral crest with respect to increased peak power consumption, when compared to the two other power modes (60W and 90W).

The surface area of the core compared to the duration of ablation, shown in Figure **13**, shows a similarly high degree of variability as shown in the displacement, load, and peak power consumed results. There is no strong trend regarding increased surface area of the core with respect to increased ablation duration and with respect to all three power-modes (30W, 60W and 90W). The surface area of the white peripheral crest compared to the duration of ablation shows a similarly high degree of variability. There is also a trend with respect to low power mode (30W), having the largest increase in surface area of the white peripheral crest with respect to duration of ablation when compared to the other two power modes (60W and 90W). The medium power mode (60W), also has a larger increase in surface area of the white peripheral crest with respect to duration of ablation when compared to (90W).

When comparing the relationship between the static load and the displacement, shown in Figure **14**, there is a positive trend with high degree of variability.

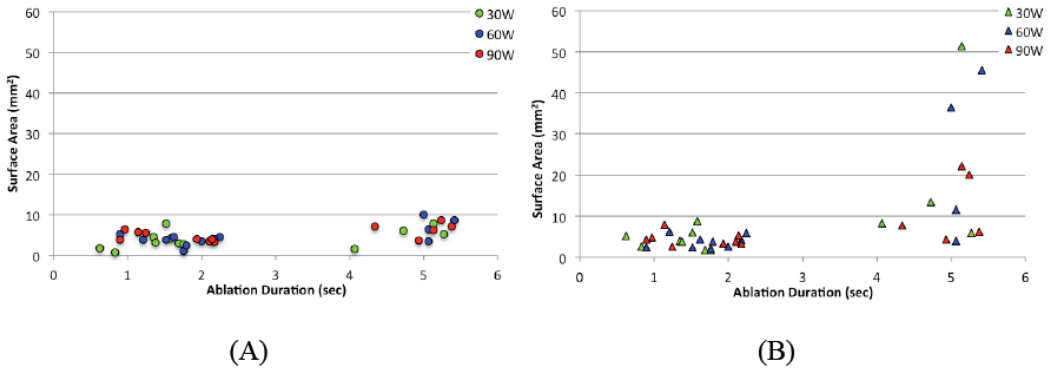

Figure 13: Surface Area of damage tissue compared with Ablation Duration (sec) for (**A**) Core and (**B**) White Peripheral Crest.

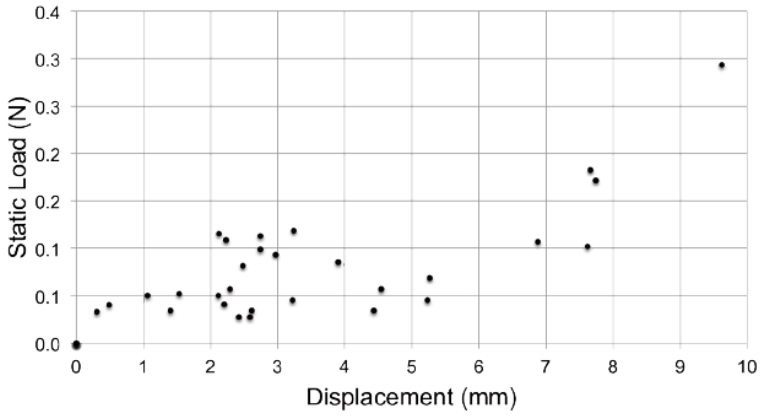

Figure 14: Static Load (N) as a function of Displacement (mm).

5. CONCLUSION

The modest sample size limited our ability to draw strong trends from comparing.

The size of the core area for all three power-modes seemed to reach a maximum, indicating the surface area of the tissue around the electrode reached its maximum value. As shown in Figure **14**, there is a high degree of variability in the force and displacement measurements. The model developed to evaluate the performance of the Hot Biopsy Forceps significantly limited our sample size and should be a focus of improvement. A more complete tissue analysis should be done in the future, which includes the depth of tissue injury and perhaps quantify the degree of protein denaturation at various muscle layers. Ultimately, the high degree of variability in the mechanical properties of tissue makes the use of force and displacement measurements difficult to be implemented as part of a control method for ablation control.

CONFLICTS OF INTEREST

The author declares no conflicts of interest associated with this manuscript.

REFERENCES

[1] Siegel R, Ma J, Zou Z, and Jemal A, 2014, “Cancer Statistics, 2014,” CA. Cancer J. Clin, 64(1), pp. 9-29. https://doi.org/10.3322/caac.21208

[2] Paspatis G. a, Vardas E, Charoniti I, Papanikolaou N, Barbatzas C, and Zois E, 2005, “Bipolar electrocoagulation vs conventional monopolar hot biopsy forceps in the endoscopic treatment of diminutive rectal adenomas,” Colorectal disease : the official journal of the Association of Coloproctology of Great Britain and Ireland, 7(2), pp. 138-42. https://doi.org/10.1111/j.1463-1318.2004.00725.x

[3] Dunkin BJ, and Joseph RA, 2010, “Lower Endoscopy,” ACS Surgery: Principles and Practice, pp. 1- 16.

[4] Panteris V, Haringsma J, and Kuipers EJ, 2009, “Colonoscopy perforation rate, mechanisms and outcome: from diagnostic to therapeutic colonoscopy,” Endoscopy, 41(11), pp. 941-51. https://doi.org/10.1055/s-0029-1215179

[5] Robert D. Tucker MD, Charles E. Platz MD, Chester E. Sievert BS, JA. Vennes MD, and Stephen E. Silvis MD. 1990, “*In vivo* Evaluation of Monopolar versus Bipolar Electrosurgical Polypectomy Snares,” *In vivo*, 85(10), pp. 1386-90.

[6] Kimmey MB, Silverstein FE, Saunders DR, and Haggitt RC. 1988, “Endoscopic bipolar forceps: a potential treatment for the diminutive polyp,” Gastrointestinal Endoscopy, 34(1), pp. 38-41. https://doi.org/10.1016/S0016-5107(88)71227-4

[7] KA. Forde, MR. Treat and JLT. 1993, “Initial clinical experience with a bipolar snare for colon polypectomy,” New York, (7), pp. 427-428. https://doi.org/10.1007/BF00311736

[8] Nath S, DiMarco JP, and Haines DE, 1994, “Basic aspects of radiofrequency catheter ablation,” J. Cardiovasc. Electrophysiol., 5(10), pp. 863-76. https://doi.org/10.1111/j.1540-8167.1994.tb01125.x

[9] Morris ML, Tucker RD, Baron TH, and Song LMWK. 2009, “Electrosurgery in Gastrointestinal Endoscopy: Principles to Practice,” Am. J. Gastroenterol, 104(6), pp. 1563-74. https://doi.org/10.1038/ajg.2009.105

[10] Investigation ANE, and City I. 1937, “Tissue Heating Accompanying Electrosurgery Experimental Investigation,” Annals of Surgery, 105(2), pp. 270-290. https://doi.org/10.1097/00000658-193702000-00014

[11] Zinder DJ. 2000, “Common myths about electrosurgery,” Otolaryngology--head and neck surgery : official journal of American Academy of Otolaryngology-Head and Neck Surgery, 123(4), pp. 450-5. https://doi.org/10.1067/mhn.2000.109758

[12] Dodde RE, Gee JS, Geiger JD, and Shih A J. 2012, “Monopolar electrosurgical thermal management for minimizing tissue damage.,” IEEE transactions on bio-medical engineering, 59(1), pp. 167-73. https://doi.org/10.1109/TBME.2011.2168956

[13] Berjano EJ. 2006, “Theoretical modeling for radiofrequency ablation: state-of-the-art and challenges for the future.,” Biomedical engineering online, 5, p. 24. https://doi.org/10.1186/1475-925X-5-24

[14] Dodde RE, Miller SF, Geiger JD, and Shih AJ. 2008, “Thermal-Electric Finite Element Analysis and Experimental Validation of Bipolar Electrosurgical Cautery,” Journal of Manufacturing Science and Engineering, 130(2), p. 021015. https://doi.org/10.1115/1.2902858

[15] Jain MK, and Wolf PD. 2000, “A three-dimensional finite element model of radiofrequency ablation with blood flow and its experimental validation,” Ann. Biomed. Eng., 28(9), pp. 1075-84. https://doi.org/10.1114/1.1310219

[16] Haemmerich D, Tungjitkusolmun S, Staelin ST, Lee FT, Mahvi DM, and Webster JG. 2002, “Finite-element analysis of hepatic multiple probe radio-frequency ablation,” IEEE transactions on bio-medical engineering, 49(8), pp. 836-42. https://doi.org/10.1109/TBME.2002.800790

[17] Khaled a-R a, and Vafai K. 2003, “The role of porous media in modeling flow and heat transfer in biological tissues,” Int. J. Heat Mass Transf., 46(26), pp. 4989-5003. https://doi.org/10.1016/S0017-9310(03)00301-6

[18] Shih TC, Kou HS, and Lin WL. 2002, “Effect of Effective Tissue Conductivity on Thermal Dose Distributions of Living Tissue with Directional Blood Flow During Thermal Therapy,” Int. Comm. Heat Mass Transf., 29(I), pp. 115-126. https://doi.org/10.1016/S0735-1933(01)00330-X

Received on 13-11-2024 Accepted on 18-12-2024 Published on 24-12-2024

https://doi.org/10.31875/2409-9848.2024.11.08